ISEIS

Journal of Environmental Informatics 45(1) 42-56 (2025)

Journal of Environmental Informatics

www.iseis.org/jei

Predictive Modeling and Optimization of Microalgae *Chlorella vulgaris* Biodiesel Production: Assessing the Performance of a Raw Biogas-Powered Diesel Engine with Diethyl Ether Blended Biodiesel

A. Ahmad[1, 2 *], A. K. Yadav[3], and A. Singh[1]

[1] *Department of Mechanical Engineering, Netaji Subhas University of Technology, New Delhi 110078, India*
[2] *Department of Mechanical Engineering, Graphic Era (Deemed to be University), Dehradun 248002, India*
[3] *Department of Mechanical Engineering, Raj Kumar Goel Institute of Technology, Ghaziabad 201017, India*

Received 13 January 2023; revised 11 June 2023; accepted 09 September 2023; published online 04 January 2025

ABSTRACT. Biodiesel production has drawn significant interest due to its potential as a renewable and environmentally favorable alternative to conventional diesel fuel. This study focuses on the prediction and optimization of biodiesel synthesis from *Chlorella vulgaris* microalgae oil using response surface methodology (RSM) and genetic algorithm (GA). The transesterification process factors, including molar ratio, catalyst concentration, reaction temperature, reaction time, and stirring speed, are explored using a Box-Behnken Design (BBD). The GA proved to be the optimal parameter combination for achieving a high biodiesel yield. Under the optimized conditions of molar ratio of 6.77:1, catalyst concentration of 1.38 wt%, reaction temperature of 65 °C, reaction time of 90 min, and stirring speed of 574 rpm, the biodiesel yield reached 98.38% (wt%). Experimental validation confirms the accuracy of the predicted results. This study also investigates the efficient use of produced biodiesel with diethyl ether as an additive and diesel blend in a dual-fuel diesel engine mode by varying the biogas mass flow rate (6, 8, and 10 L/min). Test blends of biodiesel/diesel/diethyl ether as pilot fuel and biogas as the primary fuel demonstrate satisfactory engine performance and reduced NO_x and smoke emissions compared to baseline diesel. However, carbon monoxide (CO) and hydrocarbon (HC) emissions increase. Among the tested blends, B20DEE10Bio (10) exhibited diesel-like engine performance, resulting in a 3.47% increase in brake thermal efficiency (BTE) and a 4.17% decrease in brake-specific fuel consumption (BSFC). While NO_x and smoke emissions decreased by 30.78 and 54.6%, CO and HC emissions increased by 41.27 and 37.3%, respectively, compared to baseline diesel. This research contributes to the optimization of biodiesel production and its utilization in sustainable energy systems, offering a promising pathway towards reducing environmental impacts and achieving energy security.

Keywords: Chlorella vulgaris microalgae biodiesel, biogas, genetic algorithm, optimization, dual-fuel engine, performance, emissions

1. Introduction

In an era of rapid industrialization and exponential population growth, the global demand for energy continues to escalate at an unprecedented rate. However, this surge in energy consumption comes at a hefty price, as it puts tremendous strain on our finite fossil fuel resources and contributes to environmental degradation. As a result, there is an urgent need to explore sustainable and renewable alternatives that can mitigate the detrimenttal effects of traditional energy sources (Singh et al., 2020; Manimaran et al., 2022). Biodiesel, a renewable and environmenttally friendly fuel, has emerged as a promising solution to address these challenges. Derived from organic feedstocks such as vegetable oils, animal fats, and microalgae, biodiesel offers numerous advantages over conventional fossil fuels. Not only does it significantly reduce greenhouse gas emissions, but it also offers the potential for energy security, economic growth, and sustainable development (Hoang, 2021). Biodiesel can be produced from a range of oils, including those of both edible (first-generation) and non-edible (second-generation) origins. However, the utilization of edible oils as feedstocks raises concerns regarding increased production costs and the contentious issue of food versus fuel (Balasubramanian et al., 2021). Therefore, it becomes imperative, to explore the production of biodiesel using non-consumable oils. The inefficiency of biodiesel production from first and second-generation feedstocks stems from their high production costs and the potential risks they pose to food security. Consequently, researchers have redirected their focus towards sustainable resources such as microalgae as third-generation feedstocks for biodiesel synthesis. Microalgae are recognized as a promising third-generation oil feedstock due to their ability to produce high oil yields in a short time frame and their minimal land requirements. Additionally, microalgae can be cultivated using wastewater, further enhancing their potential as a sustainable source of oil (Kumar et al., 2016). Because of its higher density as well as kinematic viscosity, the firsthand use of raw oil is restricted, so it has to be converted into their

* Corresponding author. Tel.: +918423484028; fax: 0120-2788350.
E-mail address: aqueel.me20@nsut.ac.in (A. Ahmad).

ISSN: 1726-2135 print/1684-8799 online
© 2025 ISEIS All rights reserved. doi: 10.3808/jei.202500531

respected methyl-ester (biodiesel) for proper utilization in diesel engines. The transesterification process is a viable method for the conversion of microalgae oil into biodiesel (Kusumo et al., 2017). This process is influenced by various operating parameters. Due to the varying compositions of oil feedstocks across different oil types, it is imperative to optimize process parameters when utilizing a singular oil feedstock in a specific region.

The researchers used a variety of experimental techniques to optimize process variables. These techniques included the response surface method (RSM), Taguchi approach, artificial neural network (ANN), fuzzy logic, genetic algorithms (GA), comparative design solution (CDS), screening design (SD), and regression design (RD) (Hajra et al., 2015; Marwaha et al., 2019; Zhao et al., 2022). The combination of RSM and GA has been recognized as a novel and efficacious technique for both modeling and optimization purposes (Singh et al., 2022). The RSM is a widely used optimization technique in research due to its ability to achieve optimal results with a smaller number of experiments. This is attributed to its capacity to detect a good fit, estimate errors accuratly, and provide excellent graphical analysis (Rajesh et al., 2019). The RSM technique was utilized in multiple studies to enhance the reaction parameters. Betiku et al. (2014) examined the utilization of the RSM approach for biodiesel production from sesame oil. Under optimized conditions, the transesterification method produced a maximal yield of 99.71%. These conditions included a molar ratio of 6.24, a catalyst loading of 1.04 wt%, and a reaction time of 51.09 min. The focus of the subsequent research studies was to examine the synergistic impact of combining RSM and GA in the optimization of biodiesel production. Ning et al. (2021) utilized RSM and GA to optimize the transesterification procedure for biodiesel production through palm oil. The optimal parameters for catalyst concentration, molar ratio, and transesterification temp were determined to be 8.82 wt%, 16.79:1, and 65.12 °C, respectively. By utilizing a GA optimizer, the maximum biodiesel yield was found to be 99.15%. Chizoo et al. (2022) used RSM coupled GA approach for parametric optimization of biodiesel production from waste chicken fat. Under optimal conditions of 50.21 min reaction time, 50.20 °C operating temperature, 6.9:1 methanol/fat molar ratio, and 0.78 wt% catalyst proportions, a maximum biodiesel yield of 94.89% was achieved using GA. The results demonstrate that the use of GA resulted in a 2.36% increase in biodiesel yield compared to RSM when both methods were applied under identical operating conditions.

The characteristics of the diesel engine were evaluated using optimized blends of biodiesel and diesel. Considering this context, Yatish et al. (2018) investigate the impact of biodiesel obtained from Bauhinia variegata oil on the diesel engine characteristics. The B30 blend has been observed to demonstrate comparable engine performance and combustion characteristics to that of conventional diesel fuel. The experimental results indicate that utilization of B30 blends in diesel engines leads to a significant reduction in CO and HC emissions by 47.06 and 30.23%, respectively. However, the NO_x emission was oberved to increase by 20% in comparison to diesel fuel. Similarly, Vishal et al. (2020) synthesized biodiesel using rubber seed oil as the feedstock and subsequently evaluated its engine performance. Utilization of the B10 blend indicates a correlation between BSFC and BTE, which is in closer proximity to that of diesel fuel. The emission levels of B10 exhibit a lower level in comparison to those of B20 and neat diesel fuel, respectively. Manimaran et al. (2022) analyzed the impact of biodiesel derived from waste okra seed oil on diesel engine. They observed that the B20 blend exhibited enhanced engine performance, with higher BTE (32.69%), lower BSFC (0.25 kg/kWh), reduced EGT (321 °C), and improved combustion characteristics, whereas the B20 blend exhibited lower HC (15.94%), CO (22.2%), and smoke opacity (15.62%) emissions compared to B100. However, the NO_x emissions for B20 were 2.52% lower than those of neat diesel fuel. Biodiesel exhibits a high viscosity, flash point, and cetane number as compared to diesel. The elevated oxygen content in biodiesel reduces CO, unburned HC, and VOC emissions. The slight increase in NO_x emissions can be attributed because of variations in oxygen level along with in-cylinder temperature (Marwaha et al., 2019). To address NO_x emissions in biodiesel powered CI engine, the introduction of a certain amount of gaseous fuel (biogas) with air during the intake stroke can be employed. Combining biogas and biodiesel can effectively reduce NO_x and smoke emissions while maintaining diesel-like performance. Goga et al. (2021) examined the performance and emission parameters of a dual fuel engine. This study utilized blends of rice bran oil biodiesel and diesel as pilot fuel, while raw biogas was used as the primary fuel. The study revealed an increase in BSFC and a lower BTE in dual fuel mode compared to regular diesel. However, when compared to conventional diesel, the combined use biodiesel and varying mass flow rates of biogas resulted in decreased NO_x and smoke emissions while exhibiting higher levels of HC and CO emissions.

Based on a comprehensive literature review, it has been observed that very limited studies have employed the GA technique to optimize regression equations for biodiesel production from third-generation feedstocks. Consequently, the present study aims to address this research gap by focusing on biodiesel production from *Chlorella vulgaris* microalgae oil. Moreover, it is important to note that no significant work has explored the maximization of biodiesel yield by using the RSM-coupled GA approach to optimize production parameters. In the trans-esterification procedure, this study evaluates the influence of key parameters such as molar ratio, catalyst concentration, reaction temperature, reaction time, and stirring speed, as well as their interactions, on the biodiesel yield. The RSM technique, combined with the Box-Behnken Design (BBD) method, is utilized to develop a regression equation for biodiesel production, which is subsequently optimized using the GA technique. The quality of the produced biodiesel is thoroughly evaluated and compared against the ASTM D6751 standard. Another notable contribution of this research is the exploration of the potential utilization of a ternary fuel blend (microalgae biodiesel, diethyl ether additive, and diesel) as pilot fuel, along with the use of raw biogas as the primary fuel, in diesel engines operating in dual-fuel mode. To the best of our knowledge, no prior research has focused on this specific aspect. Experimental analysis involves blending the produced microalgae biodiesel with diethyl ether additive and neat diesel at different volume frac-

tions and assessing their performance and emission characteristics with different flow rates of biogas. Furthermore, the regulated results of the diesel engine are documented and compared with standard diesel fuel. By addressing these novel aspects, this research aims to contribute valuable insights into the optimization of biodiesel production from *Chlorella vulgaris* microalgae oil, the utilization of *Chlorella vulgaris* microalgae biodiesel, diethyl ether additives, and diesel blends, and the incorporation of raw biogas as a primary fuel in diesel engines. The findings of this research have the potential to pave the way for the future development of environmentally friendly and sustainable energy solutions.

2. Materials and Method

The following section elucidates the process employed for the synthesis of biodiesel from *Chlorella vulgaris* microalgae oil. Furthermore, it outlines the methodologies stipulated by the ASTM standards, which were utilized to measure the fuel properties of the test samples. Additionally, it encompasses a comprehensive explanation of the implementation of RSM and GA for the optimization of process parameters.

2.1. Biodiesel Production and Analysis

Chlorella, a member of the Chlorophyta family, is a green microalga that exhibits the capability to thrive under autotrophic and heterotrophic conditions. Its growth relies on the presence of CO_2, water, sunlight, and trace amounts of minerals, facilitating its reproduction through photosynthesis (Kumar et al., 2016). Several *Chlorella* species have been studied for their potential in biodiesel production. These include *C. vulgaris*, *C. protothecoides*, *C. emersonii*, and *C. sorokiniana*. *Chlorella vulgaris* is a species that exhibits great potential for biodiesel production owing to its substantial lipid content (ranging from 5 to 58%) and impressive lipid productivity (measured at 1,217 mg/l/day) (Mata et al., 2010). The microalgae oil derived from *Chlorella vulgaris* species was specifically obtained from the Soley Institute in Turkey. The properties of *Chlorella vulgaris* microalgae oil were measured using established techniques (Table 1), and it was observed that the viscosity of the microalgae oil is 14.48 cSt, and the density is 0.92 g/cm³. These values indicate that microalgae oil may encounter challenges related to fuel flow in engines and may not perform similarly to diesel in terms of viscosity and density. Additionally, the high molecular weight of the oil, which is approximately 873, can lead to issues such as increased soot discharges as well as carbon deposits around the injectors. These problems necessitate regular maintenance of the affected components and may ultimately impact the thermal efficiency of the engine (Feng et al., 2012).

To mitigate the difficulties associated with soot, it becomes necessary to convert the microalgae oil into biodiesel through the process of transesterification. Transesterification helps improve the fuel properties of microalgae oil, making it a viable alternative to diesel fuel. The *Chlorella vulgaris* microalgae oil exhibited a low acid value, with an observed value of 0.2 mg KOH/g, which falls within the acceptable limit. Therefore, there is no need for esterification to decrease the acid value. The free fatty acid (FFA) content was assessed prior to the implementtation of base-catalyzed transesterification. The results indicated an FFA content of 0.1%, which falls within the acceptable range for successful transesterification. In this study, base-catalyzed transesterification was employed for the biodiesel synthesis using RSM. The transesterification process entrails the conversion of one mole of triglycerides (*Chlorella vulgaris* microalgae oil) with three moles of alcohols (CH_3OH), resulting in the formation of three moles of fatty methyl esters (*Chlorella vulgaris* microalgae biodiesel) and one mole of glycerol, as depicted in Figure 1. Raw *Chlorella vulgaris* microalgae oil and analytical-grade chemicals were utilized for all experiments outlined in the design matrix, as presented in Table 2. The catalyst concentration was achieved using potassium hydroxide (KOH) pellets expressed as a weight percentage, and methanol (99.9% purity) was utilized as the alcohol. The experimental setup was customized to meet the specifications of the design matrix, and all process parameters were meticulously controlled. In order to mitigate the potential impact of experimental errors, all experiments were conducted concurrently within a controlled environment.

The experimental apparatus comprised of a conical flask equipped with a magnetic stirrer. The flow diagram of the base-catalyzed transesterification experiment is illustrated in Figure 1. After the experimental procedure, transesterified final products were transferred to separating funnels and allowed to settle for 12 hours. Two separate phases were obtained upon equilibrium. The top layer comprised methyl ester (microalgae biodiesel), while the bottom layer consisted of crude glycerol with other suspended residual impurities. The microalgae biodiesel was purified using distilled water heated to 90 °C. Multiple washing cycles were conducted in order to eliminate any residual amounts of catalyst, methanol, and glycerol. The residual water was subjected to evaporation at a temperature of 110 °C, followed by filtration using filter paper. The biodiesel production yield was calculated using Equation (1):

$$Biodiesel\ \ Yield\,(\%) = \frac{WPMB \times 100\%}{WRMO} \tag{1}$$

where *WPMB* is the weight of the produced microalgae biodiesel; *WRMO* is the weight of the raw microalgae oil.

The fatty acid configuration of biodiesel was analyzed with the help of gas chromatography (GC) which includes a built-in flame ionization detector. 0.2 g of microalgae methyl esters were injected into the GC compartment, which was equipped with a split/split-less injection port with a split ratio of 50:1. Initially, the temperature remained at 120 °C for 2 min before increasing at a pace of 40 °C/min to its final value of 240 °C and holding at this temperature for 7 min. At an 8 mL/min flow rate, nitrogen gas was used as a carrier gas. During GC operation, five peaks of palmitic acid (C16:0), stearic acid (C18:0), oleic acid (C18:1), linoleic acid (C18:2), and linolenic acid (C18:3) were found with GC area yields of 20.68, 1.78, 38.63, 10.57, and 18.26%, respectively, as shown in Table 1.

Table 1. Properties and Fatty Acid Configuration of *Chlorella vulgaris* Microalgae Oil

Property	*Chlorella vulgaris* Oil	Fatty Acid	Degree of Unsaturation	Oil (wt%)
Density(g/cc) @ 15 ℃	0.92	Palmetic Acid	C16:0	20.68
Kinematic Viscosity (cSt) @ 40 ℃	14.48	Stearic Acid	C18:0	1.78
Acid Value (mgKOH/g oil)	0.68	Oleic Acid	C18:1	38.63
Molecular Weight (g/mol)	873.00	Linoleic Acid	C18:2	10.57
Calorific Values (MJ/Kg)	38.24	Linolenic Acid	C18:3	18.26

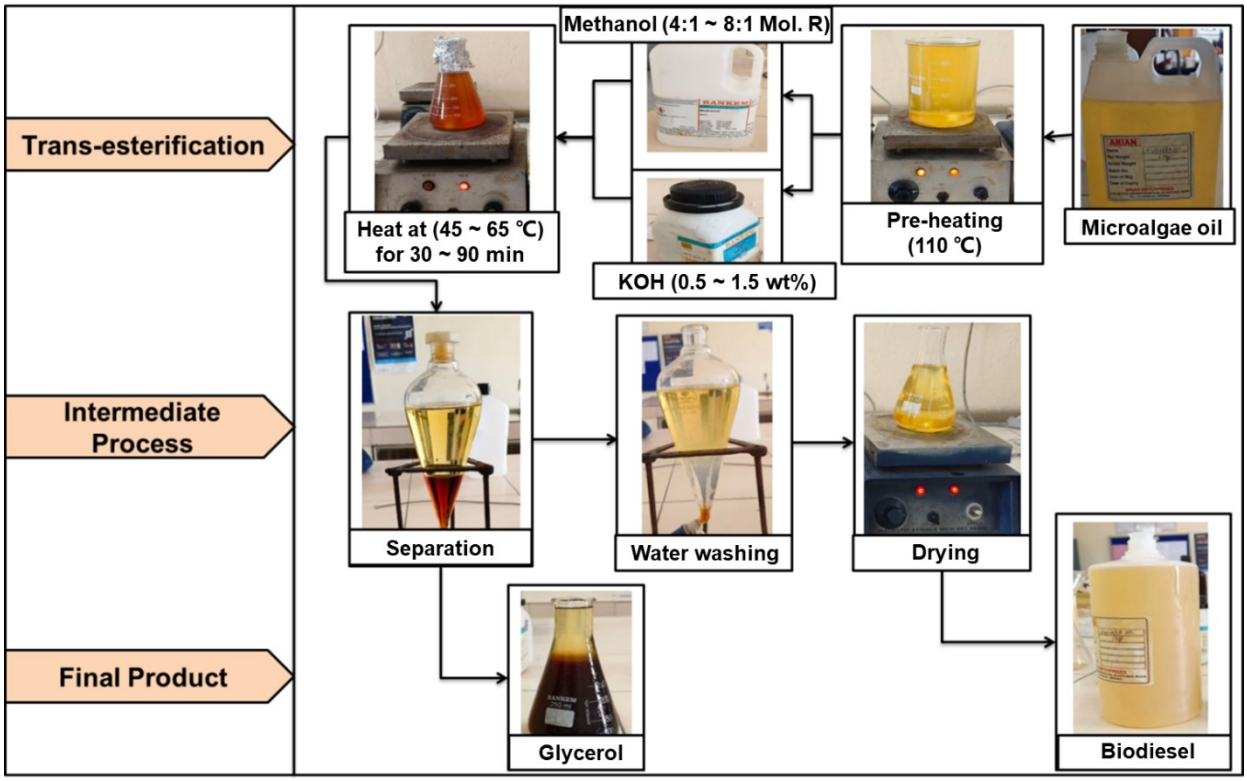

Figure 1. Trans-esterification process for microalgae biodiesel production.

2.2. Biogas Generation

Biogas is a renewable energy source characterized by its exceptional stability, lack of odor, and colorless appearance. The production of this substance occurs via the process of anaerobic digestion of biodegradable materials. The biogas employed in the study was generated by the process of anaerobic digestion, which involved a combination of cow manure and kitchen food waste. The process of biogas production was carried out utilizeing a fixed-dome biogas digester. This type of digester consists of a stable and immobile gas container positioned atop the digester structure. The preparation of the biogas feedstock involved mixing equal proportions of water and cow manure, along with a small quantity of kitchen refuse, in a mixing reservoir. Subsequently, the resulting slurry was directed into the digester container through an inlet compartment. Due to the presence of water and anaerobic microbes inside the digester, the slurry underwent anaerobic digestion. This microbial activeity led to the breakdown of complex carbon compounds present in cow manure and culinary waste, resulting in the production of simpler substances. The anaerobic disintegration of these composite carbon combinations ultimately yielded biogas, completing a cycle that typically spanned approximately two months. The level of toxicity associated with biogas is dependent on the nature of the feedstocks used in its production. When a mixture of biogas is burned, it produces a distinct blue flame, releasing a substantial amount of heat and energy. It is important to note that different biogas feedstocks result in varying chemical compositions. The presence of H_2S (hydrogen sulfide), CO_2 (carbon dioxide), and water in biogas contributes to its highly corrosive nature. The biogas produced during this process was collected in the dome-shaped top of the biogas generator and subsequently transported to the engine via pipelines. In order to sustain continuous biogas production, the consumed slurry was periodically replenished with fresh slurry. The properties of the biogas used as the test fuel were characterized according to the ASTM D6751 standard procedure, as outlined in Table 3.

2.3. Response Surface Methodology (RSM)

In the present statistical investigation, the optimization of transesterification process parameters was achieved through the

establishment of a RSM model using Design Expert software version 8.0.6. The objective was to obtain precise results with the minimum number of experimental trials, so a conventional BBD was employed. This design is known for its ability to provide accurate outcomes while minimizing the required number of experimental trials. The BBD was constructed using five numeric input factors: methanol/oil molar ratio (A), catalyst concentration (B), reaction temperature (C), reaction time (D), and stirring speed (E). Each factor was examined at three different levels, denoted as high (+1), medium (0), and low (−1), as presented in Table 2. This design facilitated the development of an experimental matrix for both data collection and subsequent optimization purposes. A total of 46 runs were conducted utilizing the BBD, which included six center points per block. These runs were utilized in the RSM model that was chosen, as described in Table S1 in Supplementary Material. To minimize the impact of random errors, the transesterification process was repeated thrice for every combination of factors. To enhance the dependability and precision of the experimental observations, several replicates were conducted Subsequently, three steps were followed in the analysis of the obtained data: (i) analysis of variance (ANOVA), (ii) regression analysis, and (iii) generating plots to visualize the output results for microalgae biodiesel synthesis. In the ANOVA step, the statistical significance of the input factors and their interactions on the response variable (biodiesel yield) was determined (Luo et al., 2021). A regression analysis was then conducted to develop a mathematical model that describes the relationship between the input factors and the biodiesel yield. This model allowed for the prediction of biodiesel yield based on the specified process parameters, facilitating the identification of optimal conditions for maximum yield. To assess the accuracy and reliability of the RSM model, the predicted biodiesel yield was compared to the corresponding experimental results.

2.4. Modeling of Genetic Algorithm (GA)

The GA is a form of stochastic non-linear optimization that falls under the umbrella of artificial intelligence. It has become increasingly popular for optimizing complex functions, as it is capable of effectively solving discontinuous fitness functions. GAs employs a regression equation as a fitness function, enabling them to surpass classical optimization approaches in various research works (Khan et al., 2022). The entire GA was executed using MATLAB, and its process flow is depicted in Figure S1. The use of GAs has increased dramatically over the past few years. Genetic algorithms provide an effective means for optimizing biodiesel yield. Their ability to handle non-linear fitness functions and their integration with other methodologies, such as RSM or neural networks, allow for enhanced biodiesel production and process optimization. In order to determine the optimum values of input procedure parameters for achieving the highest possible biodiesel yield (%), an optimization objective was addressed. The GA optimization process consisted of several crucial steps, outlined as follows:

Step 1: A random chromosomal population was generated, representing different combinations of genes.

Step 2: The genes of each chromosome were decoded, corresponding to the molar ratio (x_1), catalyst concentration (x_2), reaction temperature (x_3), reaction time (x_4), and stirring speed (x_5).

Step 3: Using RSM models, the expected biodiesel yield (%) was calculated based on the input parameters provided.

Step 4: The fitness of every single chromosome was evaluated, along with that, the highest fitness level (fit max) was also determined.

Step 5: If the fit max value was less than or equal to the required fitness level (fit required), the following genetic operations were performed: selection based on projected numerical control, crossover, and mutation. This created a new population of chromosomes, and the process continued from Step 2. If the condition was not met, the optimization process was halted. The goal of maximizing the biodiesel yield (%) was formulated as a standard mathematical problem, and the values of x_1, x_2, x_3, x_4, and x_5 were sought to maximize this objective function while adhering to the specified constraints. The constraints includeed ranges for each input parameter, such as $4{:}1 \le x_1 \le 8{:}1$, $0.5 \le x_2 \le 1.5\%$, $450 \le x_3 \le 650$ °C, $30 \le x_4 \le 90$ min, and $400 \le x_5 \le 600$ rpm.

Table 2. Selected Independent Variables and Levels

Variables	Symbols	Levels		
		−1	0	1
Methanol/Oil Molar Ratio	A	4:1	6:1	8:1
Catalyst Concentration (wt%)	B	0.5	1	1.5
Reaction Temperature (°C)	C	45	55	65
Reaction Time (min)	D	30	60	90
Stirring Speed (rpm)	E	400	500	600

Table 3. Important Properties of Produced Biogas

Properties	Value	Test Method
Chemical Composition	(65 ~ 70% CH_4, 35 ~ 40% CO_2, volume)	
Density at 1 atm. (kg/m^3)	1.2	D3585
Lower Heating Value (MJ/kg)	26.4	D1940
Auto Ignition Temperature (°C)	604 ~ 644	-
Octane Number	132	D2696
Energy Content (KW/m$^{3)}$	5.2 ~ 5.8	D4870
Flame Speed (m/s)	24	D7428

2.5. Engine Setup and Experimental Procedure

The experiment was conducted using a single-cylinder, four-stroke, variable compression ratio (VCR) diesel engine. The engine specifications can be found in Table S2, and Figure 2 provides a graphical representation of the test rig. To maintain consistency during the trial, the engine was sustained at a steady speed of 1,500 rpm. Temperatures were measured at different locations using K-type thermocouples, which included intake air, exhaust gas, and lubricating oil. The measurement of standard pilot fuel was facilitated using a standard buret and timer. The engine underwent modifications to enable its operation in dual fuel mode, which has been previously applied to various fuels

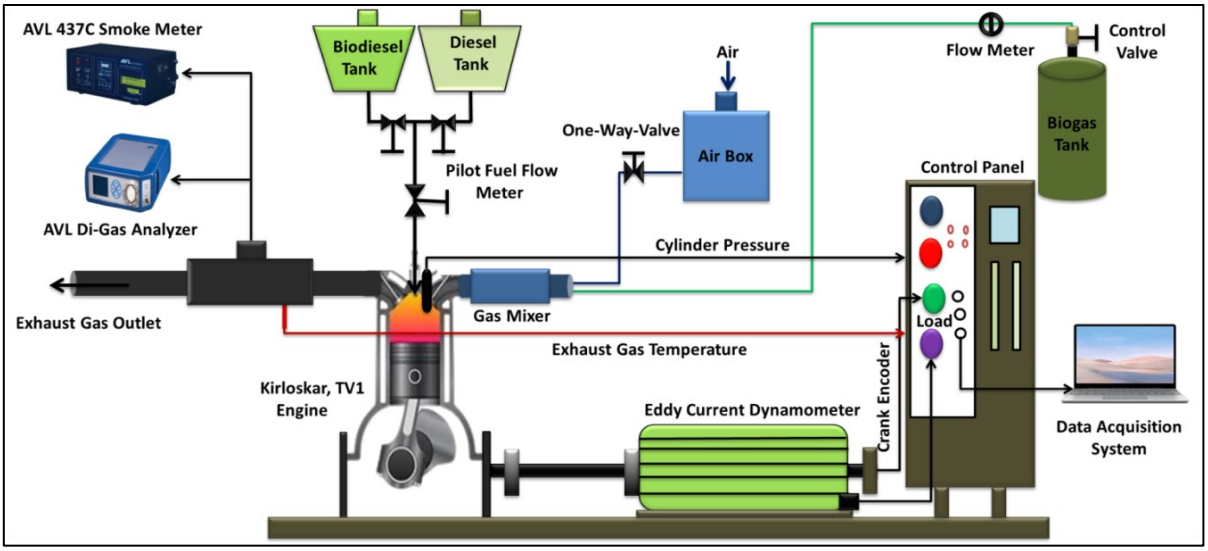

Figure 2. Layout of experimental setup.

to evaluate their respective engine responses. In the experimental setup, the flow rate of biogas was regulated using a flow meter. The diagram presented in Figure 2 depicts the integration of a gas mixer positioned ahead of the inlet manifold. This is done to guarantee a uniform combination of air and biogas prior to its introduction into the engine cylinder. The mixing device follows the carburetion principle, employing a venturi with biogas intake bores around the throat to achieve the desired mixture. At the downstream end of the venturi, turbulent flow promotes thorough mixing of biogas with incoming air. The venturi design allows biogas to be drawn from the biogas cylinder due to the pressure drop at the throat. The design of the air-biogas mixer takes into account various factors, such as velocities at the throat and inlet, throat diameter, angles of the converging and diverging sections, and the diameter and angle of the biogas fuel inlet holes. The emissions of gaseous constituents consist of CO, HC, and NO_x were measured utilizing an AVL DIGAS 444-N gas analyzer. Additionally, a diesel smoke meter (AVL 437C) was used to determine the smoke opacity. Prior to commencing the experiments, a thorough inspection of the test engine is conducted, encompassing parameters such as temp, water, and lubricating oil flow, as well as fuel tank levels. In order to establish a stable operating condition, the test engine is allowed to run for 15 min. Subsequently, a careful examination is performed to verify the adequacy of water as well as lubrication oil circulation, and the calibration of the dynamometer loading error is conducted. Once the test engine reaches a state of steady operation, the diesel and various blends [D100, B20, B20DEE10, B20DEE10Bio (6), B20DEE10Bio (8), B20DEE10Bio (10)], are subjected to analysis under diverse load conditions.

3. Results and Discussion

3.1. Identification and Analysis of RSM Model

To determine the ideal conditions for biodiesel production, a quadratic function was chosen as the model. The suitability of the quadratic model was assessed using the coefficient of determination (R^2) and the Fischer test. The R^2 provides a measure of how well the model fits the experimental data, while the Fischer test evaluates the statistical significance of the model (Yatish et al., 2018). The statistical significance of the model was assessed by evaluating both the *F*-value and the *P*-value. The *F*-value represents the ratio of the mean square of the regression to the mean square of the residual, while the *P*-value indicates the significance level associated with the *F*-value. A lower *P*-value suggests a higher degree of significance for the model (Sharma et al., 2022). To analyze the biodiesel yields, an analysis of variance (ANOVA) was performed, and the results are presented in Table S4. The significance of the model was determined based on its *F*-value, which was calculated to be 49.456. This value indicates that the model is statistically significant, with a probability of occurrence due to random variation or noise of only 0.01%. In the context of statistical significance, model terms with *P*-values below 0.05 are considered to be statistically significant. In order to ensure the reliability of the model, a lack-of-fit analysis was conducted. Specifically, terms A, B, C, D, E, AC, AB, BC, A^2, B^2, and D^2 were found to be statistically significant in this particular analysis. A lack of fit is considered statistically insignificant when compared to pure error, indicating that the model adequately represents the dataset. The lack of fit *F*-value of 0.5713 further supports this conclusion. The overall predictability of the model was evaluated using the R^2 value. A higher R^2 value, closer to 1, indicates better predictability, while a value closer to 0 suggests a less accurate fit to the experimental data. In this study, the R^2 value was found to be 0.975, which is considered acceptable. Additionally, the adjusted R^2 value was 0.955, and the predicted R^2 was 0.914. The small discrepancy among these values indicates a good correspondence between the model and the experimental findings, allowing for an accurate prediction of biodiesel yield. The coefficient of variation (CV%) was 0.924, indicating a high level of measurement precision and reliability in the conducted tests. The software equations recommended for biodiesel yield pre-

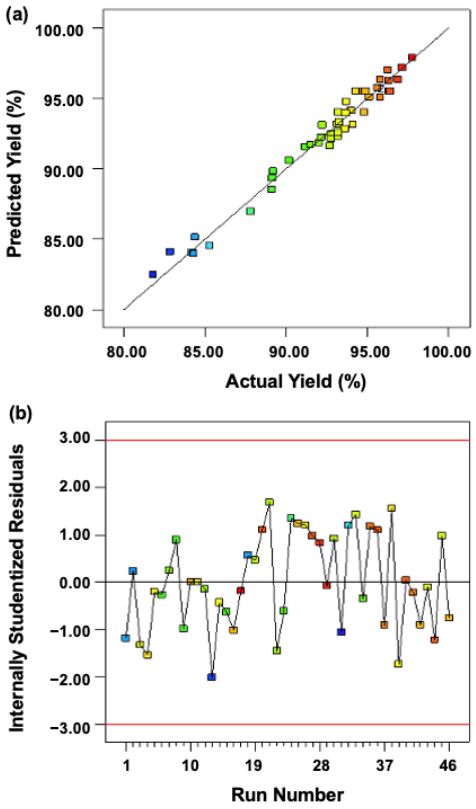

Figure 3. (a) Predicted verses actual biodiesel yield; (b) residual verses run for biodiesel yield.

diction are presented in Equation (2). Figure 3(a) illustrates a comparison between the actual biodiesel yield values and their predicted values, demonstrating minimal disparity and accurate prediction by the quadratic model. Furthermore, Figure 3(b) displays a residual vs. run plot, showing that the residuals are randomly dispersed and indicating consistent variance across all tests. Overall, the analysis confirms the significance and reliability of the chosen model, supporting its effectiveness in predicting biodiesel yield based on the experimental data:

$$\begin{aligned} Yield\ (\%) = {} & 15.90635 + 21.59469A + 2.37458B - 0.24123C \\ & - 0.13522D + 0.040221E - 1.36604A^2 - 7.59667B^2 \\ & + 0.0044083C^2 - 0.00156D^2 - 0.00002583E^2 \\ & - 0.29750AB - 0.058AC + 0.031292AD \\ & - 0.002887AE + 0.162BC + 0.037167BD \\ & + 0.01135BE + 0.001991CD - 0.0001CE \\ & + 0.000073DE \end{aligned} \quad (2)$$

3.2. Effect of Process Parameter on Biodiesel Yield

The present investigation aimed to analyze the impact of different process parameters within predetermined ranges. The experimental conditions were varied in order to examine the impact on the reaction outcome. Specifically, the molar ratio was varied within the range of 4:1 to 8:1, the catalyst concentration was varied between 0.5 ~ 1.5 wt%, the reaction temperature was varied between 45 ~ 65 °C, the reaction duration was ranged from 30 to 90 min, and the stirring speed was altered within the range of 400 to 600 rpm. We utilized KOH as the catalyst due to its low corrosiveness, and methanol was chosen as the alcohol due to its costeffectiveness. To analyze the significance of these parameters, statistical analysis was conducted under four different conditions. For each analysis, three parameters were held constant while the remaining two were varied. The results were represented through surface plots, as shown in Figure 4. The results of the ANOVA analysis presented in Supplementary Table 4 indicate that the molar ratio and reaction time were among the most significant attributes, while the reaction temperature, catalyst concentration, and stirring speed had a comparatively lower impact on the yield. The investigation revealed that the molar ratio is a crucial factor that significantly impacts the yield. The results indicate [Figures 4(a) ~ 4(c)] that an increase in molar ratios led to a corresponding increase in the rate and efficacy of ester conversion. The 3D surface plot depicted in Figure 4(a) showcases the variation of the molar ratio and catalyst concentration. The experimental conditions were maintained at a fixed temperature of 55 °C, a reaction time of 60 min, and a stirring speed of 500 rpm. We observed a production yield of over 96% when the molar ratio was between 6:1 and 7:1, with a close to 1 wt% catalyst concentration. However, a reduction in yield was observed when the molar ratio increased from 7:1 to 8:1, which could be attributed to surplus methanol diminishing the catalyst's effectiveness (Visha et al., 2020). The data presented in Figures 4(d) and 4(e) illustrates the impact of varying catalyst concentrations. The results indicate that there is a positive correlation between the concentration of the catalyst and the recovery of Ester. Specifically, an increase in catalyst concentration from 0.5 to 1.0% resulted in an increase in Ester recoveries. However, the trend reversed beyond 1% and a significant drop in Ester recoveries was observed near 1.5%. The observed reduction in performance at elevated concentrations of KOH could potentially be attributed to the generation of soap compounds (Rajesh et al., 2019). Regarding the reaction temperature, Figures 4(b) and 4(d) showed that an increase in temperature initially led to improved biodiesel yield. However, beyond a certain limit, the yield started to decrease. This decrease was attributed to the boiling temperature of methanol (64.5 °C), causing evaporation and reducing the availability of reactants. Therefore, the maximum yield was achieved just before the saturation temperature. Increased reaction time was found to enhance biodiesel productivity. Longer reaction times allowed for the completion of the transesterification reaction. Figure 4(e) demonstrated that a higher catalyst concentration required more time to complete the reaction. Shorter reaction times combined with higher catalyst concentrations resulted in a reduced yield. The stirring speed exhibited a notable influence on the reaction rate, with higher speeds resulting in enhanced conversion of free fatty acids (FFAs). This observation suggests that increased turbulence facilitated a more effective molecular-level interaction between the reactants. Moreover, higher agitation levels reduced the hindrance encountered during mass transfer, consequently accelerating the reaction rate and promoting greater FFA conversion (Bhuiya et al.,

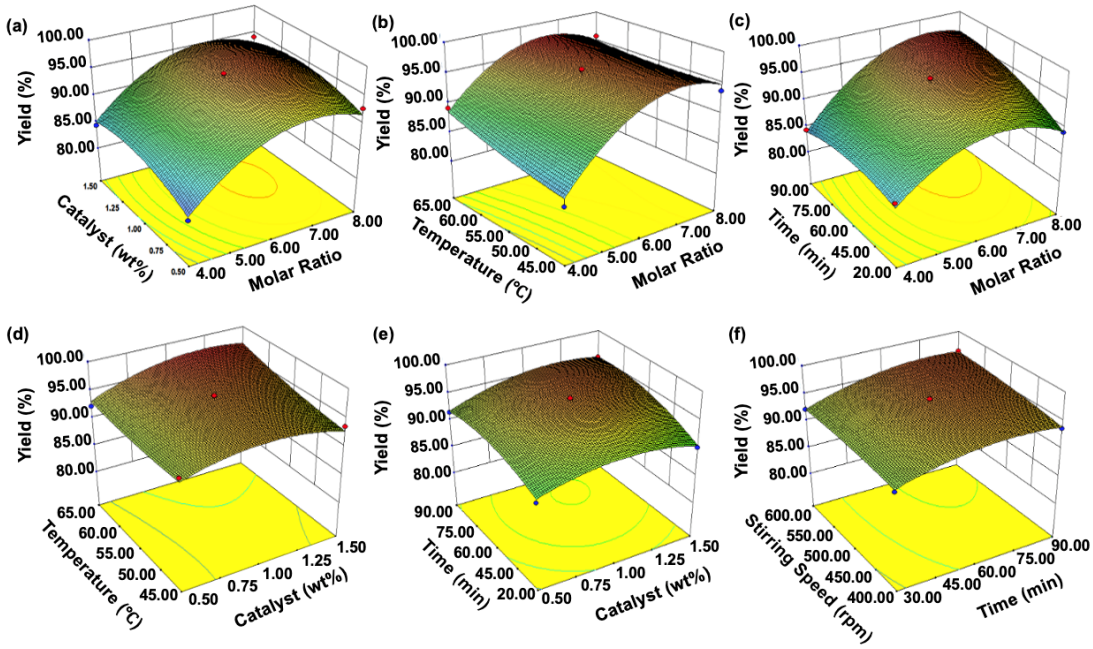

Figure 4. 3D surface graphs for *Chlorella vulgaris* biodiesel yield with the combined impact of (a) molar ratio and catalyst concentration, (b) molar ratio and temperature, (c) molar ratio and time, (d) catalyst concentration and the temperature, (e) catalyst concentration and the time, and (f) time and stirring speed.

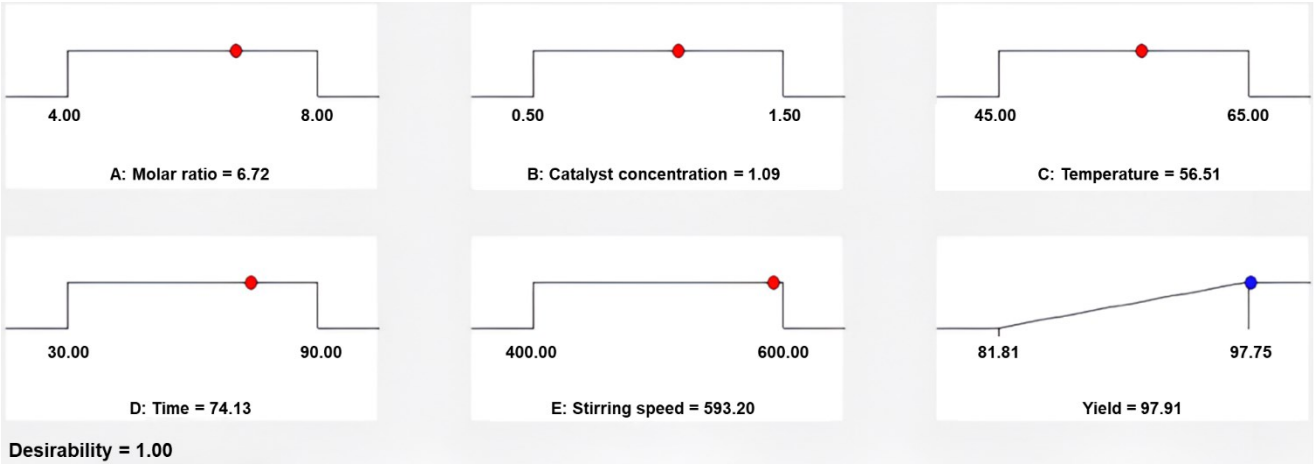

Figure 5. Optimized result by RSM.

2020). However, it is important to note that excessively high agitation speeds, surpassing 600 rpm, might lead to a decline in FFA conversion. This reduction can be attributed to the limited interaction time between the reactants caused by the extreme agitation conditions. The corresponding relationship between yield and stirring speed is graphically depicted in Figure 4(f).

3.3. Optimization of Biodiesel Production

3.3.1. RSM Approach

The present study employed a desirability approach to enhance the process of biodiesel synthesis. Within the Design of Experiments (DOE) software, a range of optimization methods were available for consideration. In this study, numerical optimization, widely recognized as the most effective approach for continuous optimization, was chosen to maximize the production of biodiesel. To achieve an optimal response, the study focused on varying the molar ratios, catalyst concentrations, reaction temperatures, reaction times, and stirring speeds. By systematically exploring the effects of these process variables on biodiesel yield, the study aimed to identify the combination of parameters that would yield the highest possible biodiesel production. The desirability function, a mathematical tool used to evaluate multiple response variables simultaneously, was employed to generate a single value representing the overall desirability of specific process conditions. Through the application

of this function, it was determined that the highest attainable biodiesel yield is 97.91%. To achieve this optimal yield, specific parameter values were identified, including a molar ratio of 6.72:1, a catalyst concentration of 1.09 wt%, a reaction temperature of 56.51 °C, reaction duration of 74.13 min, and a stirring speed of 593.20 rpm. These parameter values were assigned a desirability score of 1.00 (Figure 5) indicating their significance in maximizing the biodiesel yield. In order to validate the optimization outcomes, additional experimentation was conducted by specifying independent variables for the RSM method. Confirmatory experiments were carried out using the optimal parameter combinations to assess the accuracy of the predictions made during the optimization process. It is noteworthy that the highest observed error rate between the predicted and experimental values was 1.57%, indicating a relatively small deviation.

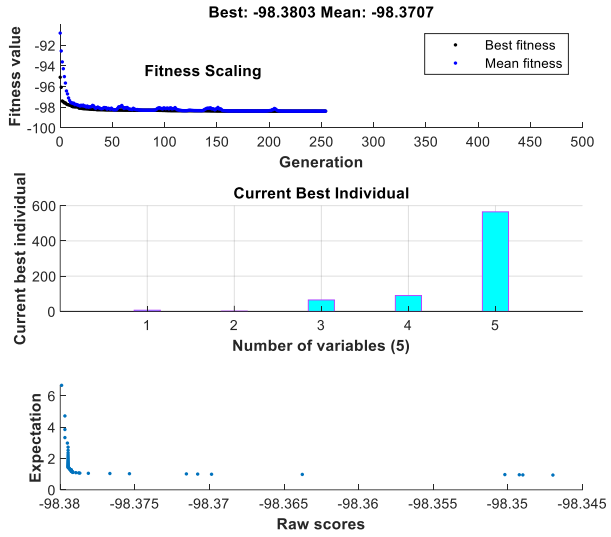

Figure 6. Results of best fitness, mean fitness, current best individual, and expected yield.

3.3.2. Genetic Algorithm Approach

To facilitate the optimization process, a mathematical equation was constructed within the GA framework to represent the objective function. Additionally, RSM was employed to establish correlations between the input parameters and the response metrics. Based on the experimental data obtained from BBD, a quadratic RSM model was constructed to describe the response surface. This model achieved a 95% confidence level and was created using RSM capabilities within the DOE software. The GA optimization incorporated the bound values of the input process parameters, defining their maximum and minimum limits. The GA's key parameters, such as mutation rate, population size, generations, and crossover rate, were carefully set to ensure effective optimization. Fitness functions, as defined in Equation (3), played an important role in evaluating the fitness of the chromosomes during the GA optimization process. The GA program provided optimal results in terms of both the best and mean values, as depicted in Figure 6. Additionally, the best individuals were identified centered on the quantity of variables. Overall, the utilization of the GA optimization approach, along with RSM modeling, facilitated the identification of optimal input process parameters for maximizing biodiesel yield (%). The GA's parameter settings and the comparison between experimental and GA results provided valuable insights into the effectiveness of the optimization process:

$$\begin{aligned}\text{Fitness function} = -\big(&15.90635 + 21.59469\times x_1 + 2.3745\times x_2\\ &- 0.13522\times x_4 + 0.040221\times x_5\\ &- 0.29750\times x_1\times x_2 - 0.058\times x_1\times x_3\\ &+ 0.031292\times x_1\times x_4 - 0.002887\times x_1\times x_5\\ &+ 0.162\times x_2\times x_3 + 0.037167\times x_2\times x_4\\ &+ 0.01135\times x_2\times x_5 + 0.001991\times x_3\times x_4\\ &- 0.0001\times x_3\times x_5 + 0.000073\times x_4\times x_5\\ &- 1.36604\times x_1^{\,2} - 7.59667\times x_2^{\,2}\\ &+ 0.0044083\times x_3^{\,2} - 0.00156\times x_4^{\,2}\\ &- 0.00002583\times x_5^{\,2}\big) \end{aligned} \quad (3)$$

3.3.3. Confirmation Experiment

To validate the optimization results, a rigorous validation process was conducted by performing confirmation experiments using the input parameters obtained from both RSM and GA methods. These experiments aimed to verify the accuracy and reliability of the optimization products. Through the confirmatory tests using the best parameter combinations identified by the optimization methods, it was observed that the predictions made by the models were highly accurate and consistent with the experimental results. This validation step provided strong evidence supporting the reliability and effectiveness of the optimization approaches employed. By utilizing different optimization strategies, the ideal circumstances for biodiesel production were determined. Table 4 displays the optimal input process attributes estimated by the GA method, which led to a remarkable biodiesel yield (%) of approximately 98.38%. This yield surpassed the results achieved using the a priori approach of RSM. Both methods demonstrated their efficacy; however, the parameter combination derived from the GA approach proved to be the most favorable in accordance with the objectives of the study. Hence, it can be confidently regarded as the optimal set of circumstances for biodiesel production.

3.5. Physicochemical Properties of Microalgae Biodiesel

The production of biodiesel as an alternative fuel for diesel engines necessitates adherence to fuel standards to ensure its quality and suitability for use. To evaluate the excellence of biodiesel, various physical and chemical properties were calculated and compared to the criteria specified by the ASTM standards. Table 5 provides a comprehensive overview of the physiochemical characteristics of microalgae oil, biodiesel, and conventional diesel. Biodiesel is noteworthy for its viscosity that falls within the conventional diesel range, which facilitates seamless engine operation and enhances engine durability. Additionally, it should be noted that the flash point of biodiesel exhibits a significant increase, thereby contributing to the im-

Table 4. Validation Test

Method	Molar Ratio	Catalyst Concentration (wt%)	Reaction Temperature (°C)	Reaction Time (min)	Stirring Speed (rpm)	Predicted Yield (%)	Experimental Yield (%)	Error (%)
RSM	6.72:1	1.09	56.51	74.13	593.2	97.91	96.37	1.57
GA	6.77:1	1.38	65	90	574.6	98.38	97.12	1.28

Table 5. Physiochemical Properties of Produced Biodiesel

Properties	Biodiesel	Diesel	Diethyl Ether	Test Methods	EN/14214 Limit	ASTM/ D6751 Limit
Density @15 °C (g/cm^3)	0.85	0.83	0.71	D4052	0.86 ~ 0.90	-
Viscosity @ 40 °C (cSt)	3.8	3.0	0.3	D445	3.5 ~ 5.0	1.9 ~ 6.0
Flash Point (°C)	124	75	–40	D93	Min 120	Min 130
Pour Point (°C)	–11	−18	–38	D97	-	–15 ~ –16
Cetane Number	51	49	125	D613	Min 51	Min 47
Iodine Value (mgI_2/100 g)	90	120	-	EN14214	Max 120	-
Acid Value (mg KOH/g oil)	0.23	0.08	0.06	D664	Max 0.5	Max 0.5
Oxidation Stability (h)	11.7	17.3	-	EN14112	-	Min 3 h
Calorific Value (MJ/kg)	40.7	44.2	33.9	D240	-	-

provement of safety measures during its transportation. The high oxidation stability of biodiesel is another notable feature, indicating that it can be stored for an extended period without experiencing a significant decline in fuel quality. Additionally, the favorable cold flow properties of biodiesel facilitate better operability and ensure smooth engine performance even under low-temperature conditions. These attributes collectively contribute to the overall suitability and effectiveness of biodiesel as an alternative fuel for diesel engines. The analysis of the physiochemical characteristics and compliance with stringent standards underscores the viability and reliability of microalgae biodiesel, further supporting its potential as a sustainable and high-quality fuel option in the context of diesel engine applications.

3.6. Effect of Ternary Fuel Blends and Biogas Flow Rate on Engine Characteristics

This study comprehensively investigated the performance and emission characteristics of a diesel engine through the utilization of various fuel blends of diesel, microalgae biodiesel, and diethyl ether additives as pilot fuels and biogas as primary fuel. All experimental tests on the engine were conducted at a constant speed of 1,500 revolutions per minute (rpm), covering a range of brake power outputs from 0 to 5.2 kilowatts (kW). The injection timing was consistently set at 23 degrees before top dead center (TDC), while the compression ratio stood at 17.5.

3.6.1. Brake Thermal Efficiency (BTE)

Figure 7(a) illustrates the variation in brake thermal efficiency (BTE) with respect to brake power, comparing different fuel blends against diesel as the reference. The inclusion of a 20% microalgae biodiesel blend exhibits a negative impact on engine performance. The observed phenomenon can be explained by the lower heating value and higher kinematic viscosity of the fuel, which have a negative impact on the atomization and combustion processes (Barik et al., 2017). The B20 blend exhibits a noteworthy decrease in BTE, specifically up to 4 ~ 5% at the rated brake power of 5.2 kW, due to unfavorable fuel properties. The incorporation of diethyl ether as an admixture in the biodiesel/diesel blend at a concentration of 10% has been found to yield favorable outcomes with respect to enhanced combustion characteristics. The observed improvement results in a rise of 0.5 ~ 1.2% in BTE throughout the engine's complete operating range. It is worth noting that, in general, the use of a biodiesel/diesel blend as the pilot fuel alongside biogas as the primary fuel results in lower BTE. This can be attributed to the decrease in the calorific value of biodiesel and biogas, which exert a greater influence on BTE. Nonetheless, the incorporation of diethyl ether as an additive in pilot fuel blends by 10% and an increase in biogas flow rate up to 10 L/min are favorable factors that contribute to improved combustion characteristics and engine performance. These optimizations lead to a BTE improvement ranging from 0.87 to 3.47% at full load. Diethyl ether, biodiesel, and diesel blends exhibit a slightly lower cetane number, which in turn facilitates enhanced fuel/air mixing. This improved mixing capability enables more efficient energy release, thereby enhancing combustion efficiency as well as BTE (Barik and Murugan, 2016). Notably, when the biogas mass flow rate is increased from 8 to 10 L/min with B20DEE10 pilot fuel blend, a corresponding increase in BTE of 1.89 and 6.24% is observed at full load.

3.6.2. Brake Specific Fuel Consumption (BSFC)

Figure 7(b) presents the BSFC of a diesel engine using various test fuels at different levels of brake power. BSFC is defined as the amount of energy consumed (in MJ) to produce one unit of work (in kWh) at the output shaft of the engine. Under zero-load conditions, the fuel consumption rate remains invariant irrespective of the fuel blend utilized, as the power output is only utilized to overcome the internal friction of the engine (Khayum et al., 2021). At idle running of the engine, BSEC is higher for B20 due to their lower calorific values. Additionally, the higher mass density of B20 fuel compared to other fuels results in a higher fuel mass burn per unit cycle for the same volume of fuel injection in comparison to diesel fuel (Bora et al., 2016). However, at moderate and higher engine brake power levels, the combustion efficiency of B20 fuel de-

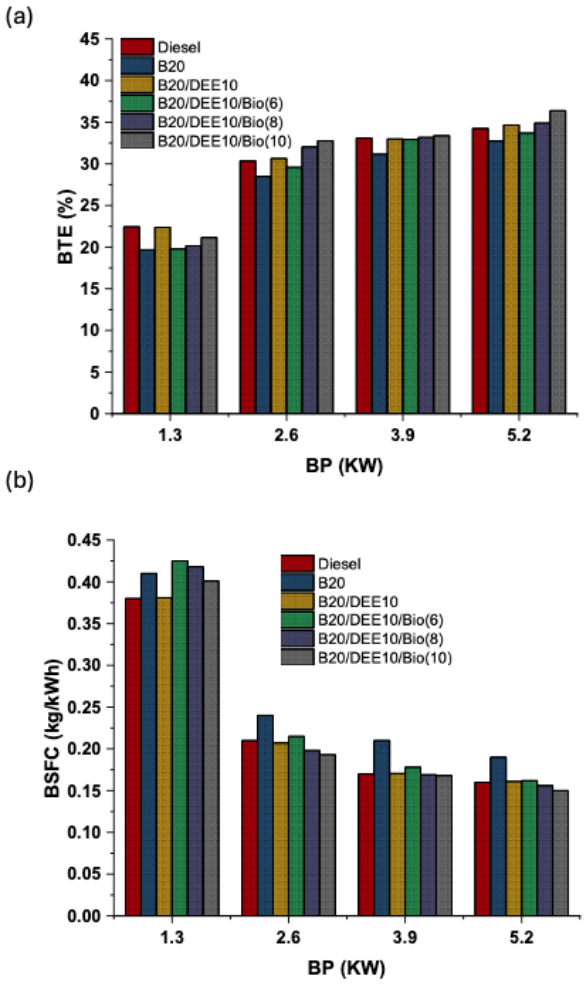

Figure 7. (a) Variation of BTE with BP; (b) variation of BSFC with BP.

creases, leading to an increase in BSEC of 14.28 ~ 18.75%, respectively, when compared to diesel fuel. On the other hand, the addition of diethyl ether to the fuel blends offers favorable properties such as density, viscosity, and atomization, resulting in improved combustion and reduced energy consumption for the same power output (Barik and Murugan, 2016). It is noteworthy that the diethyl etherblend fuels demonstrate similar BSEC values as diesel fuel. Furthermore, the addition of diethyl ether as an additive in pilot fuel blends by 10% and an increase in biogas flow rate up to 10 L/min contribute to enhanced combustion characteristics and engine performance. These optimizations lead to a decrease in BSFC ranging from 1.17 to 4.17% at full load.

3.6.3. Carbon Monoxide (CO)

Figure 8(a) depicts the impact of changes in fuel blend composition on carbon monoxide (CO) emissions. CO is a hazardous gas formed as a result of incomplete combustion within the engine cylinder (Sharon et al., 2012). The graph reveals that the B20 fuel blend exhibits reduced CO emissions compared to diesel fuel. Notably, the ternary blend B20DEE10 demonstrates a significant reduction in CO emissions of 21 to 25% across the entire engine operating range. This reduction can be attributeed to the higher availability of oxygen for combustion due to the addition of diethyl ether to the fuel blends (Goga et al., 2021). Furthermore, it was observed that the introduction of gaseous fuel, specifically a rising quantity of biogas mass flow rate, resulted in elevated CO emissions. This can be attributed to the affluent air-fuel mixture associated with the utilization of gaseous fuel, which leads to an inadequate provision of oxygen required for complete combustion (Thakkar et al., 2021). Additionally, it is noteworthy that the ternary blend B20DEE10Bio (10) resulted in a substantial increase in CO emissions by 41.27% at the rated power of 5.2 kW.

3.6.4. Hydrocarbon (HC)

Figure 8(b) depicts the relationship between unburned hydrocarbon (UHC) emissions and brake power. The utilization of a biodiesel blend (B20) demonstrates a noteworthy reduction in unburned hydrocarbon (UHC) emissions, ranging from 3.4 to 5.5% across all loading conditions. This decrease can be attributed to the higher availability of oxygen facilitated by biodiesel's oxygen content. However, an excessive increase in biodiesel blend concentration may lead to higher UHC emissions due to the elevated viscosity, which can hinder spray penetration and result in larger fuel droplets with reduced surface area for effective combustion (Yatish et al., 2018). To overcome these challenges, the incorporation of diethyl ether proves beneficial by improving combustion characteristics and thereby reducing the release of unburned hydrocarbons. The introduction of diethyl ether to biodiesel/diesel blends contributes to a 6.78% reduction in UHC emissions compared to pure diesel fuel at full load conditions. Under all testing conditions, it is observed that UHC emissions are higher in dual-fuel operations compared to pure diesel, B20, and B20DEE10 operations. This can be attributeed to the poorer combustion characteristics associated with the dual-fuel mode. Factors such as reduced flame velocity, the presence of carbon dioxide, reduced oxygen concentration, and the longer ignition delay of biogas contribute to this outcome (Goga et al., 2021). While biodiesel and diethyl ether blended with diesel have the potential to reduce hydrocarbon emissions due to their higher oxygen concentrations, the influence of biogas on overall hydrocarbon emissions remains significant. Notably, the ternary blend B20DEE10Bio (10) exhibits a substantial increase in HC emissions by 37.32% at the rated power of 5.2 kW.

3.6.5. Nitrogen Oxide (NO_x)

The nitrogen oxides (NO_x) formation is known to be influenced by factors such as surplus availability of oxygen and temperature. It has been stated that NO_x formation initiates expeditiously at in-cylinder temperatures above 1,500 K and increases further with higher temperatures and the oxygen content in the fuel. Hence, NO_x formation is dependent on the concentration of oxygen, the in-cylinder temperature, and the residence time of gases at temperatures exceeding 1,500 K. Figure 8(c) illustrates the relationship between NO_x emissions of all fuel blends

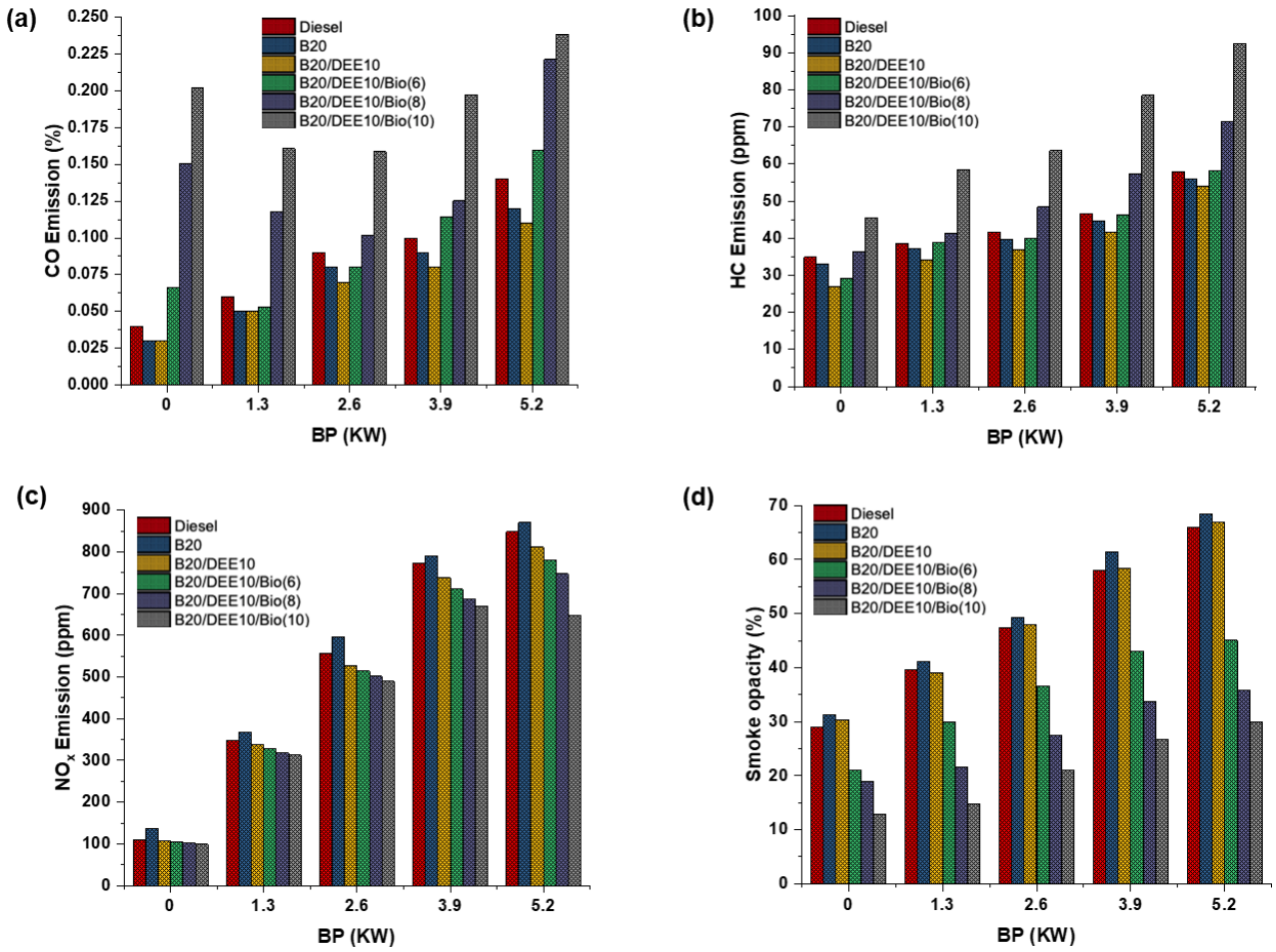

Figure 8. Variation of (a) load vs. CO, (b) load vs. HC, (c) load vs. NO_x, and (d) load vs. smoke opacity.

across diverse engine load conditions. It is evident that the B20 fuel blend exhibits the highest NO_x emissions, ranging from 24 to 26% higher compared to pure diesel across the entire operating range. This increase can be attributed to the slower burning rate and higher heat release characteristics of B20, which promote NO_x formation. Similar observations were made by Sharon et al. (2012), who noted an increment in NO_x emissions as the fraction of palm biodiesel burned towards the end of the combustion cycle as a result of the elevated molecular weight of the biodiesel fraction in the blend. In contrast, the ternary blend B20DEE10 demonstrates a reduction in NO_x emissions ranging from 2.9 to 4.5% across the entire load range compared to pure diesel. The introduction of diethyl ether in the fuel blends contributes to this reduction (Arunkumar et al., 2019). Furthermore, the addition of biogas to the combustion chamber leads to a decrease in NO_x emissions due to the absence of oxygen. It was also observed that NO_x emissions decrease at a faster rate with increasing biogas flow rates, attributed to the presence of carbon dioxide (CO_2). The presence of CO_2 in biogas lowers the peak cylinder temperature as it possesses a higher specific heat capacity (Chhabra et al., 2016). Moreover, fuels blended with diethyl ether exhibit lower gas temperatures at the completion of combustion, which aids in the reduction of NO_x generation. The NO_x emission degradation rate for the BD20-DEE10Bio (10) blend was found to be 30.78% compared to pure diesel at rated power.

3.6.6. Smoke Opacity

The inadequate supply of oxygen within the combustion chamber leads to incomplete fuel combustion, resulting in the generation of smoke. However, alternative fuels such as biogas, biodiesel, and diethyl ether have been recognized for their ability to produce lower smoke emissions compared to diesel. The relationship between smoke opacity and brake power is depicted in Figure 8(d), revealing that biogas and biodiesel/diethyl ether blends contribute to a reduction in smoke opacity, particularly in dual-fuel mode. Interestingly, the presence of methane, a significant component of biogas, aids in lowering smoke emissions when oxygenated fuels such as biodiesel and diethyl ether are used, compared to conventional diesel. The smoke emissions exhibit a consistent decrease when utilizing the B20DEE10 blend, which can be attributed to the high oxygen content in diethyl ether, facilitating more complete combustion. Consequently, alcohol-based fuels like diethyl ether hold promise as clean substitute fuels when blended with diesel in various proportions (Mahla et al., 2019). Furthermore, Figure

Table 6. Comparative Analysis

Fuel Type	Engine Used	Performance Characteristics	Emission Characteristics	References
Biogas-diesel/DEE/KME	Kirloskar TAF 1, single cylinder, air cooled 4-stroke diesel engine	BTE$^{\uparrow}$, BSFC$^{\downarrow}$, VE$^{\downarrow}$	HC$^{\downarrow}$, CO$^{\downarrow}$, $NO_x$$^{\uparrow}$, smoke emission$^{\uparrow}$	Barik and Murugan (2016)
Biogas-rice bran biodiesel	Single-cylinder, direct injection, naturally aspirated, water-cooled, VCR diesel engine	-	HC$^{\downarrow}$, CO$^{\downarrow}$, $NO_x$$^{\uparrow}$, $CO_2$$^{\uparrow}$	Bora and Saha (2016)
Biogas-diesel/KME	Kirloskar TAF 1, single cylinder, air cooled 4-stroke diesel engine	BSFC$^{\uparrow}$, EGT$^{\downarrow}$, BGES$^{\downarrow}$	$NO_x$$^{\downarrow}$, smoke emission$^{\downarrow}$	Barik et al. (2017)
Biogas-rice bran biodiesel/diesel	Kirloskar Single cylinder air cooled 4 stroke diesel engine	BTE$^{\downarrow}$, BSFC$^{\uparrow}$	$NO_x$$^{\downarrow}$, smoke emission$^{\downarrow}$, CO$^{\uparrow}$, HC$^{\uparrow}$	Goga et al. (2021)
Biogas-rice bran biodiesel/n-butanol/diesel	Kirloskar single cylinder air cooled 4 stroke diesel engine	BTE$^{\downarrow}$	CO$^{\uparrow}$, HC$^{\uparrow}$, $NO_x$$^{\downarrow}$, smoke opacity$^{\downarrow}$	Goga et al. (2021)
Biogas-spirulina microalgae Biodiesel/n-butanol/diesel	Single-cylinder, direct injection, water-cooled, VCR diesel engine	BTE$^{\uparrow}$, BSFC$^{\downarrow}$	$NO_x$$^{\downarrow}$, smoke emission$^{\downarrow}$, HC$^{\uparrow}$, CO$^{\uparrow}$	Ahmad et al. (2023)
Biogas-*Chlorella vulgaris* microalgae biodiesel/DEE/diesel	Kirloskar single cylinder, water-cooled, VCR diesel engine	BTE$^{\uparrow}$, BSFC$^{\downarrow}$	$NO_x$$^{\downarrow}$, smoke emission$^{\downarrow}$, HC$^{\uparrow}$, CO$^{\uparrow}$	Present Survey

10(d) demonstrates that increasing the flow rate of biogas from 6 to 10 L/min results in diminished smoke formation, potentially due to the absence of aromatic compounds found in biogas. When employing biogas as the primary fuel, significant reductions in smoke emissions are observed. Specifically, smoke emissions decrease by 31.5, 45.56, and 54.6% for the BD20-DEE10Bio (6), BD20DEE10Bio (8), and BD20DEE10Bio (10) blends, respectively.

3.7. Comparative Analysis of Experimental Findings

The experimental findings obtained in this study were subjected to a comprehensive comparison with the results of related research studies, as presented in Table 6. The operating parameters of a biodiesel-biogas-powered diesel engine were meticulously examined in relation to our current findings. Remarkably, our findings demonstrate a remarkable resemblance in engine performance while showcasing a substantial decrement in emission levels in comparison to the results reported in other research studies.

4. Conclusions and Future Scope

This study focuses on the production of biodiesel from *Chlorella vulgaris* microalgae oil, with a specific emphasis on optimizing process parameters using the response surface methodology (RSM) technique in conjunction with the genetic algorithm (GA). The results demonstrate that the parametric combination derived from GA outperforms that obtained from RSM, resulting in a remarkable maximum biodiesel yield of 98.54% (wt%) under the optimized conditions. The analysis of variance (ANOVA) identifies the molar ratio and reaction time as the most influential parameters, followed by the reaction temperature, catalyst concentration, and stirring speed. Furthermore, the produced biodiesel complies with the ASTM specifications for fuel properties. In terms of engine performance and emissions, test blends comprising diesel/biodiesel/diethyl ether as the pilot fuel and biogas as the primary fuel exhibit satisfactory performance while reducing NO_x and smoke emissions compared to the baseline diesel. However, carbon monoxide (CO) and hydrocarbon (HC) emissions have increased relative to diesel. Among the tested blends, the B20DEE10Bio (10) blend demonstrates engine performance and fuel combustion characteristics similar to diesel. This blend yields a notable 3.47% increment in brake thermal efficiency and a significant 4.17% decrement in brake-specific fuel consumption. While NO_x and smoke emissions reduces by 30.78 and 54.6%, correspondingly, CO and HC emissions rises by 41.27 and 37.32%. The addition of diethyl ether as an additive in the biodiesel/diesel blend leads to a reduction in cylinder temperature at the end of combustion. Simultaneously, the use of biogas as the primary fuel limits oxygen availability, resulting in a substantial decrease in NO_x emissions compared to baseline diesel. After thorough experimenttation, it can be concluded that the B20DEE10 ternary fuel blend, combined with a biogas flow rate of 10 L/min, emerges as the optimal blend ratio due to its superior performance and emission characteristics when compared to other tested fuels.

In summary, the use of biogas and a ternary fuel blend in diesel engines has shown potential for improving performance, reducing emissions, and decreasing reliance on fossil fuels. Future research endeavors may focus on further optimizing the blend ratios and investigating the impacts of different biogas compositions, along with exploring advanced emission control technologies to mitigate CO and HC emissions. Additionally, studying the long-term effects of these fuel blends on engine durability and the overall environmental impact would be valuable for comprehensive evaluation and validation in real-world applications.

Acknowledgments. The authors wish to thank the Raj Kumar Goel Institute of Technology for providing the research facilities necessary to conduct this work, and the Netaji Subhas University of Technology for providng the softwater support used in this research.

References

Ahmad, A., Yadav, A. K., Singh, A. and Singh, D. K. (2023). Enhancement of biogas yield from dual organic waste using hybrid statistical

approach and its effects on ternary fuel blend (biodiesel/n - butanol/diesel) powered diesel engine. *Environ. Prog. Sustain. Energy*, 42(5), e14163. https://doi.org/10.1002/ep.14163

Arunkumar, M., Kannan, M. and Murali, G. (2019). Experimental studies on engine performance and emission characteristics using castor biodiesel as fuel in CI engine. *Renew. Energy*, 131, 737-744. https://doi.org/10.1016/j.renene.2018.07.096

Balasubramanian, D., Hoang, A.T., Venugopal, I.P., Shanmugam, A., Gao, J. and Wongwuttanasatian, T. (2021). Numerical and experimental evaluation on the pooled effect of waste cooking oil biodiesel/diesel blends and exhaust gas recirculation in a twin-cylinder diesel engine. *Fuel*, 287, 119815. https://doi.org/10.1016/j.fuel.2020.119815

Barik, D. and Murugan, S. (2016). Effects of diethyl ether (DEE) injection on combustion performance and emission characteristics of Karanja methyl ester (KME)-biogas fueled dual fuel diesel engine. *Fuel*, 164, 286-296. https://doi.org/10.1016/j.fuel.2015.09.094

Barik, D., Murugan, S., Sivaram, N.M., Baburaj, E. and Sundaram, P.S. (2017). Experimental investigation on the behavior of a direct injection diesel engine fueled with Karanja methyl ester-biogas dual fuel at different injection timings. *Energy*, 118, 127-138. https://doi.org/10.1016/j.energy.2016.12.025

Betiku, E. and Adepoju, T.F. (2013). Methanolysis optimization of sesame (*Sesamum indicum*) oil to biodiesel and fuel quality characterization. *Int. J. Energy Environ. Eng*., 4, 1-8. https://doi.org/10.1186/2251-6832-4-9

Bhuiya, M.M.K., Rasul, M.G., Khan, M.M.K. and Ashwath, N. (2020). Biodiesel production and characterisation of poppy (*Papaver somniferum* L.) seed oil methyl ester as a source of 2nd generation biodiesel feedstock. *Ind. Crop. Prod*., 152, 112493. https://doi.org/10.1016/j.indcrop.2020.112493

Bora, B.J. and Saha, U.K. (2016). Experimental evaluation of a rice bran biodiesel-biogas run dual fuel diesel engine at varying compression ratios. *Renew. Energy*, 87, 782-790. https://doi.org/10.1016/j.renene.2015.11.002

Chhabra, M., Sharma, A. and Dwivedi, G. (2017). Performance evaluation of diesel engine using rice bran biodiesel. *Egypt. J. Petrol.*, 26(2), 511-518. https://doi.org/10.1016/j.ejpe.2016.07.002

Chizoo, E., Augustine, S.C., Chukwu, E.G. and Gerald, U. (2022). Adaptive neuro-fuzzy inference system-genetic algorithm versus response surface methodology-desirability function algorithm modelling and optimization of biodiesel synthesis from waste chicken fat. *J. Taiwan Inst. Chem. Eng*., 136, 104389. https://doi.org/10.1016/j.jtice.2022.104389

Feng, Q., Jalali, A., Fincham, A.M., Wang, Y.L., Tsotsis, T.T. and Egolfopoulos, F.N. (2012). Soot formation in flames of model biodiesel fuels. *Combust. Flame.*, 159(5), 1876-1893. https://doi.org/10.1016/j.combustflame.2012.01.003

Goga, G., Chauhan, B.S., Mahla, S.K., Dhir, A. and Cho, H.M. (2021). Combined impact of varying biogas mass flow rate and rice bran methyl esters blended with diesel on a dual-fuel engine. *Energy Sources Part A-Recovery Util. Environ. Eff*., 43(1), 120-132. https://doi.org/10.1080/15567036.2019.1623948

Goga, G., Singla, V., Mahla, S.K., Chauhan, B.S., Dhir, A., Balasubramaniam, D. and Singla, N. (2021). Effects of ternary fuel blends (diesel-biodiesel-*n*-butanol) on emission and performance characteristics of diesel engine using varying mass flow rates of biogas. *Energy Sources Part A-Recovery Util. Environ. Eff.*, 1-14. https://doi.org/10.1080/15567036.2021.1910754

Hajra, B., Sultana, N., Pathak, A.K. and Guria, C. (2015). Response surface method and genetic algorithm assisted optimal synthesis of biodiesel from high free fatty acid sal oil (*Shorea robusta*) using ion-exchange resin at high temperature. *J. Environ. Chem. Eng*., 3(4), 2378-2392. https://doi.org/10.1016/j.jece.2015.08.015

Hoang, A.T. (2021). Prediction of the density and viscosity of biodiesel and the influence of biodiesel properties on a diesel engine fuel supply system. *J. Mar. Eng. Technol*., 20(5), 299-311. https://doi.org/10.1080/20464177.2018.1532734

Khan, T.A., Khan, T.A. and Kumar Yadav, A. (2022). A hydrodynamic cavitation-assisted system for optimization of biodiesel production from green microalgae oil using a genetic algorithm and response surface methodology approach. *Environ. Sci. Pollut. Res*., 29(32), 49465-49477. https://doi.org/10.1007/s11356-022-20474-w

Khayum, N., Anbarasu, S. and Murugan, S. (2021). Optimization of fuel injection parameters and compression ratio of a biogas fueled diesel engine using methyl esters of waste cooking oil as a pilot fuel. *Energy*, 221, 119865. https://doi.org/10.1016/j.energy.2021.119865

Kumar, M. and Sharma, M.P. (2016). Optimization of transesterification of *chlorella protothecoides* oil to biodiesel using box-behnken design method. *Waste Biomass Valori*., 7, 1105-1114. https://doi.org/10.1007/s12649-016-9485-5

Kusumo, F., Silitonga, A.S., Masjuki, H.H., Ong, H.C., Siswantoro, J. and Mahlia, T.M.I. (2017). Optimization of transesterification process for *Ceiba pentandra* oil: A comparative study between kernel-based extreme learning machine and artificial neural networks. *Energy*, 134, 24-34. https://doi.org/10.1016/j.energy.2017.05.196

Luo, B., Huang, G.H., Yao, Y., An, C.J., Zhang, P. and Zhao, K. (2021). Investigation into the influencing factors and adsorption characteristics in the removal of sulfonamide antibiotics by carbonaceous materials. *J. Clean Prod*., 319, 128692. https://doi.org/10.1016/j.jclepro.2021.128692

Mahla, S.K. and Dhir, A. (2019). Performance and emission characteristics of CNG-fueled compression ignition engine with *Ricinus communis* methyl ester as pilot fuel. *Environ. Sci. Pollut. Res*., 26(1), 975-985. https://doi.org/10.1007/s11356-018-3681-8

Manimaran, R., Venkatesan, M. and Kumar, K.T. (2022). Optimization of okra (*Abelmoschus esculentus*) biodiesel production using RSM technique coupled with GA: Addressing its performance and emission characteristics. *J. Clean Prod*., 380, 134870. https://doi.org/10.1016/j.jclepro.2022.134870

Marwaha, A., Rosha, P., Mohapatra, S.K., Mahla, S.K. and Dhir, A. (2019). Biodiesel production from *Terminalia bellerica* using eggshell-based green catalyst: An optimization study with response surface methodology. *Energy Rep.*, 5, 1580-1588. https://doi.org/10.1016/j.egyr.2019.10.022

Mata, T.M., Martins, A.A. and Caetano, N.S. (2010). Microalgae for biodiesel production and other applications: A review. *Renew. Sust. Energ. Rev.*, 14(1), 217-232. https://doi.org/10.1016/j.rser.2009.07.020

Ning, Y.L., Niu, S.L., Wang, Y.Z., Zhao, J.L. and Lu, C.M. (2021). Sono-modified halloysite nanotube with $NaAlO_2$ as novel heterogeneous catalyst for biodiesel production: Optimization via GA_BP neural network. *Renew. Energy*, *175*, 391-404. https://doi.org/10.1016/j.renene.2021.04.135

Rajesh, Y., Kolakoti, A., Sheakar, B.C. and Bhargavi, J. (2019). Optimization of biodiesel production from waste frying palm oil using definitive screening design. *Int. J. Eng. Sci. Technol.*, 11(2), 48-57. https://doi.org/10.4314/ijest.v11i2.4

Sharma, P., Sahoo, B.B., Said, Z., Hadiyanto, H., Nguyen, X.P., Nižetić, S., Huang, Z., Hoang, A.T. and Li, C., 2023. Application of machine learning and Box-Behnken design in optimizing engine characteristics operated with a dual-fuel mode of algal biodiesel and waste-derived biogas. *Int. J. Hydrog. Energy*, 48(18), 6738-6760. https://doi.org/10.1016/j.ijhydene.2022.04.152

Sharon, H., Karuppasamy, K., Kumar, D.S. and Sundaresan, A. (2012). A test on DI diesel engine fueled with methyl esters of used palm oil. *Renew. Energy*, 47, 160-166. https://doi.org/10.1016/j.renene.2012.04.032

Singh, N.K., Singh, Y. and Sharma, A. (2022). Optimization of biodiesel synthesis from Jojoba oil via supercritical methanol: A response surface methodology approach coupled with genetic algorithm. *Biomass Bioenerg.*, 156, 106332. https://doi.org/10.1016/j.biombioe.2021.106332

Singh, N.K., Singh, Y., Sharma, A. and Abd Rahim, E. (2020). Prediction of performance and emission parameters of Kusum biodiesel based diesel engine using neuro-fuzzy techniques combined with genetic algorithm. *Fuel*, 280, 118629. https://doi.org/10.1016/j.fuel.2020.118629

Thakkar, K., Kachhwaha, S.S., Kodgire, P. and Srinivasan, S. (2021). Combustion investigation of ternary blend mixture of biodiesel/n-butanol/diesel: CI engine performance and emission control. *Renew. Sust. Energ. Rev.*, 137, 110468. https://doi.org/10.1016/j.rser.2020.110468

Vishal, D., Dubey, S., Goyal, R., Dwivedi, G., Baredar, P. and Chhabra, M. (2020). Optimization of alkali-catalyzed transesterification of rubber oil for biodiesel production & its impact on engine perfor-mance. *Renew. Energy*, 158, 167-180. https://doi.org/10.1016/j.renene.2020.05.136

Yatish, K.V., Lalithamba, H.S., Suresh, R. and Hebbar, H.H. (2018). Optimization of bauhinia variegata biodiesel production and its performance, combustion and emission study on diesel engine. *Renew. Energy*, 122, 561-575. https://doi.org/10.1016/j.renene.2018.01.124

Zhao, K., Huang, G.H., Luo, B. and Wu, Y.W. (2022). A factorial interval chance-constrained diet model for dairy farms under climate change: A case study for the Province of Saskatchewan, Canada. *J. Clean Prod*., 360, 132059. https://doi.org/10.1016/j.jclepro.2022.132059